Button Antenna on Textiles for WLAN on Body Applications

B. Sanz-Izquierdo, J. C. Batchelor, and M. I. Sobhy.

Button Antenna on Textiles for WLAN on Body Applications

B. Sanz-Izquierdo, J. C. Batchelor, and M. I. Sobhy.

The University of Kent, Canterbury, Kent, CT2 7NT

Email: b.sanz@kent.ac.uk; j.c.batchelor@kent.ac.uk; m.i.sobhy@kent.ac.uk

ABSTRACT

A design of a wearable antenna for WLAN applications is presented in this paper. The antenna consists of a button shape outer cylindrical structure and an internal central via connected to a top disc at one end and the metal ground plane at the other. The overall size and shape achieved are those of a standard metal jeans button which camouflages the antenna for wearable applications. The rigidness of the structure is greater than for previous wearable button antenna developments. The proposed wearable antenna is designed for 2.4 GHz and 5 GHz with monopole type radiation patterns at each band. This allows for transmission to other worn devices on the body. An investigation into the measured permittivity of cotton denim is presented and a section on the equivalent circuit modelling of the antenna and the fabric is given.

Keywords — Wearable Antennas, Dual band antennas, WLAN, Pervasive computing.

1.0 INTRODUCTION:

The rapid development of wireless communication standards, including Bluetooth, WIFI, UWB, and ZigBee in recent years has contributed to the convergence of wireless and wired networks. At the same time electronic systems are becoming increasingly compact, lightweight and mobile in nature.

In light of the above, much interest has been shown in wearable computing devices which are becoming a fast growing field in application-oriented research. For instance, the provision of a wide range of user information via a body worn sensor system has already been demonstrated in the WearNET system [1].

The rapid development of wearable computing systems is driving a need for suitable body antennas. Wearable antennas have been developed in the form of conducting microstrip patches of on textile fabric [2, 3]. These were linearly polarized and probe fed. Later, microstrip feed lines were used to create circular polarization as reported in [4] while providing a feed that was conformal to the body surface for comfort. Recently, the authors of this manuscript introduced a wearable button antenna [5-7] which consisted of a top loaded monopole mounted on a dielectric over a ground plane. The flexible textile fastener Velcro was used as the dielectric substrate.

In this paper we expand on the work presented in [8] which introduced a new design of a button antenna with significant enhancements to those reported in [5-7]. Additional to [8], this paper contains measured

radiation patterns for all 3 principal planes, considerably more theory for the permittivity measurement of the clothing fabric and an equivalent lumped element circuit for the antenna and its feed. The new antenna structure differs from those in [5-7] as it is dielectric filled which reduces the overall size. There is also a top loading element which is connected directly to the ground plane. With these changes, the overall size of the structure is reduced by 23% compared to [5-7] while maintaining the dual band operation and bandwidths of the original design. It should also be noted, that the objective here is to produce an antenna with a structure disguised as a button, so its final shape is predetermined to a certain extent and we are not seeking an ultra low profile design. A further benefit of the inclusion of a dielectric within the monopole is to increase its robustness which is an obvious concern for wearable technology. Additionally, the new structure may be suitable for riveting through a textile, using a similar process to a normal jeans button. The antenna is fed by a microstrip line mounted on Velcro and covers the 2.45 GHz, 5.25 GHz and 5.5 GHz bands necessary for Bluetooth and WLAN technologies. As the button antenna is to be directly mounted on clothing fabric, a study of the permittivity of cotton denim will be presented here. The antenna has been modelled as an equivalent circuit with lumped elements and the textile fabric has been accounted for. Results are given for the modelling work which have been derived from measurement.

This paper is organized as follows: section 2 introduces the new lower profile button antenna and discusses its design and operation. Section 3 contains measurements of the dielectric constants of the textiles that the antenna and the feed are likely to be mounted on, Section 4 presents an equivalent circuit of the antenna which is derived from measured scattering parameters. Finally, Section 5 concludes the paper.

2.0 REDUCED SIZE DUAL BAND BUTTON ANTENNA

Single and Dual band metal button antennas suitable for communication in the 2.4GHz and 5GHz bands were introduced in [5-7] where a methodical description of their operation is available. The principal dimensions of the new button geometry introduced here are shown in Fig. 1 and Table 1. The antenna is a small top loaded hollow cylindrical monopole of height h_2, with a capacitively coupled centre piece which connects to the ground plane. Note that this antenna is different to that reported in [5-7] in that the centre via pin connects the top disc to the ground plane. This makes the resulting structure physically strong and raises the possibility of riveting the antenna to clothing. The total height of the centre element is $h_1+h_2+h_3$. The space between the inner and outer conductors is filled with dielectric to reduce the size and improve rigidity. The antenna is fed by a microstrip line. The total visible height of the antenna is 7.5mm and the maximum diameter is 17mm. The antenna is placed on a Velcro® substrate of height h_1 with a flexible metal ground plane on the rear side of the material. Velcro was chosen due to its flexibility and superior

Antenna parameter	Value	Electrical Length, λ (2.45GHz)	Electrical Length , λ (5.5GHz)
d_1	12.4 mm	0.101	0.230
d_2	7.0 mm	0.057	0.130
d_3	16.4 mm	0.118	0.271
d_4	14.6 mm	0.133	0.304
d_5	2 mm	0.016	0.037
h_1	1.8 mm	0.015	0.033
h_2	7.4 mm	0.060	0.137
h_3	1.5 mm	0.013	0.028
ε_{r1}	1.37	-	-
ε_{r2}	2.2	-	-
Thickness of discs	0.7 mm	0.006	0.013
Feed line width	7.0 mm		
Feed line Z_0	50Ω	-	-
Ground plane	60 mm×60mm	0.487^2	1.113^2

TABLE1: Dimensions of Dual Band Button

resistance to compression when compared to other clothing fabrics; however, any low permittivity textile material could be used with only a small retuning necessary.

All simulations presented in this paper were obtained from CST Microwave Studio.

It is not the subject of this paper to present a detailed design study of the antenna as details of a parametric study of a related structure were published in [6 & 7]. However, as reported in [8], to summarize the tuning procedure: the upper frequency band is primarily determined by the diameter of the lower disc, d_3, while the lower frequency is set by the upper disc diameter, d_4. The cylinder height, h_2, affects both bands. Secondary tuning is achieved by varying the cylinder diameters d_2 and d_5. Simulations were carried out initially with a Perfect Electric Conductor of 50mm×50mm below the antenna and then the presence of the human body was accounted for by including a three layer tissue representation, [9] beneath the ground plane. Minor retuning was necessary when the antenna was mounted on a human body. The simulated design was validated by S_{11} measurement with an Anritsu ME7808A vector network analyzer and radiation patterns were taken in a far field anechoic chamber.

The simulated and measured -10dB S_{11} values are shown in Fig.2 and Table 2 where the percentage fractional bandwidths are also given. All WLAN systems within the 2.4GHz and 5GHz ISM bands are

	Lower band		Upper band	
	frequency (MHz)	fractional bandwidth	frequency (MHz)	fractional bandwidth
Simulated on air	2415-2515	4%	4580-6275	31 %
Measured on air	2350-2515	7%	4990-6140	21%
Simulated on body	2340-2520	7%	4640-6256	30%
Measured on body	2300-2510	9%	4970-6200	22%

TABLE 2: Measured and simulated S_{11} bandwidths of the Button Antenna

matched. The radiation patterns were measured in an anechoic chamber and are given in Fig.3. The antenna was mounted on an adult male at waist height. Reasonably good omni-directionality is observed and gains of 2.65dBi at 2.45GHz, 4.6dBi at 5.25GHZ and 5.1dBi at 5.5GHz were measured. The z-axis (boresight) is normal to the user's body which means that wireless connection may be made between the button antenna and other body worn devices.

3.0 MEASUREMENT OF PERMITTIVITY OF TEXTILES

In order to design wearable antennas, the properties of textiles at microwave frequencies must be determined. The first property to be determined is the dielectric constant. We have used a transmission method for the measurement and placed the material at the centre of a rectangular waveguide supported by expanded polystyrene foam. The scattering parameters of the structure with and without the textiles are compared to determine the dielectric constant and the loss tangent. The advantages of this method are:

- The material is supported by the foam and can be accurately placed in the waveguide.
- Since this is a comparison measurement, any mismatch or inaccuracies in the measurements are subtracted.
- The length of the material sample can be increased at will to obtain a bigger difference between the two measurements and thus increase the accuracy.
- Unlike a resonance method, the measurement can be performed over a wide band of frequencies between the cut-off frequencies of the TE_{10} and the TE_{01} modes.

The method has been used to determine the dielectric constants and loss tangents of Velcro and Denim. With reference to Fig. 4, in the transverse direction we have a waveguide with equivalent width of λ_g where λ_g is the wavelength of the propagating mode in the longitudinal direction. Thus λ_g represents the cut-off wavelength of the transverse guides.

At the interface in the transverse direction we have

$$Y_1 = -jY_{01}\cot\left(\frac{\beta_1(d-a)}{2}\right) \text{ and } Y_2 = jY_{02}\tan\left(\frac{\beta_2 d}{2}\right) \qquad (1)$$

$$\beta_1 = \frac{2\pi}{\lambda_1}\sqrt{1-(\lambda_1/\lambda_g)^2} \quad ,$$

$$\beta_2 = \frac{2\pi}{\lambda_2}\sqrt{1-(\lambda_2/\lambda_g)^2} \ ,$$

$$\lambda_1 = \lambda_0/\sqrt{\varepsilon_1} \ , \quad \lambda_2 = \lambda_0/\sqrt{\varepsilon_2} \qquad (2)$$

and λ_g is the cut-off wavelength of the guide with the dielectric.

The characteristic admittances Y_{01} and Y_{02} are given by

$$Y_{01} = \frac{1}{\eta_1}\sqrt{1-(\lambda_1/\lambda_g)^2} \text{ and } Y_{02} = \frac{1}{\eta_2}\sqrt{1-(\lambda_{21}/\lambda_g)^2} \qquad (3)$$

where $\eta_1 = \sqrt{\mu_0/\varepsilon_1}$ and $\eta_2 = \sqrt{\mu_0/\varepsilon_2}$.

For propagation to be sustained, resonance must be achieved and we have $Y_1 + Y_2 = 0$ and substituting (2) and (3) we get

$$\sqrt{k^2\varepsilon_r - \beta^2}\tan(d\sqrt{k^2\varepsilon_r - \beta^2}/2) = \sqrt{k^2-\beta^2}\cot((a-d)\sqrt{k^2-\beta^2}/2) \qquad (4)$$

where k is the propagation constant in medium 1, $\beta = 2\pi/\lambda_g$ is the propagation constant in the guide with the dielectric and $\varepsilon_r = \varepsilon_2/\varepsilon_1$. If either or both dielectric media are lossy, then ε_1 and/or ε_2 are complex and β in (4) is replaced by $\gamma = \alpha + j\beta$.

For the measurement procedure: the sample is inserted in a C-band waveguide and the transmission parameters S_{21} with and without the sample are measured in amplitude and phase. The measured phase of S_{21} with and without the sample are ϕ_1 and ϕ_2 respectively, where $\phi_1 > \phi_2$ due to the dielectric. The measured phase also includes phase shift due to the length occupied by the sample, any extra length of waveguide, the waveguide to coaxial transitions and the cables connecting to the network analyser. If the

same length of waveguide and all the other components are used with and without the sample, then the difference between the two phase shifts will give us the extra phase due to the sample.

Thus $\phi_1 = \theta_1 + \theta_e$ and $\phi_2 = \theta_2 + \theta_e$ where θ_e is the extra phase shift due the measurement components, θ_1 is the phase shift due to the dielectric sample and θ_2 is the phase shift of the length of waveguide where the sample was placed but after it has been removed. The angles θ_1 and θ_2 are related to the guided wavelengths by $\theta_1 = 2\pi l / \lambda_g$ and $\theta_2 = 2\pi l / \lambda_{g0}$ where λ_g and λ_{g0} are the guide wavelengths with and without the sample.

From measurement of the difference $\Delta\phi$ between the phase angles ϕ_1 and ϕ_2 we calculate λ_g from

Material	Relative Permittivity	Loss Tangent
Velcro	1.34	6×10^{-3}
Dry Denim	1.8	7×10^{-2}

TABLE 3: Measured Relative Permittivity and Loss Tangent of Velcro and Dry Denim

$$\lambda_g = \frac{\lambda_{g0}}{1 - \Delta\phi\lambda_{g0} / 2\pi l} \qquad (5)$$

The attenuation constant is calculated from the ratio of the amplitude of S_{21} with and without the sample. When both λ_g and α are known, equation (4) is used to calculate ε_r.

Fig. 5 and Table 3 give the results for Velcro and dry denim. The small fluctuation for the permittivity of denim at 4GHz is due to residual inaccuracies in the measurement.

4.0 EFFECT OF INCLUDING THE TEXLIE MATERIALS

Next we study the effect of including the textile material parameters as measured in Section 3.0. Fig. 6 shows a comparison of the amplitude of S_{11} when Denim and Velcro are included in the simulation. It is obvious that accurate measurements of the dielectric properties of the textiles are needed and should be included in designing and optimising the antenna. The denim material decreased the resonant frequency of the lower band compared to Velcro by 4% and the higher band by 8%.

5.0 EQUIVALTENT CIRCUIT FOR BUTTON ANTENNA

An equivalent circuit for the antenna structure is valuable when designing antennas and optimizing their performance. From the equivalent circuit the radiation resistance can be identified and the power response of the antenna can be plotted. The equivalent circuit is derived by inspecting the physical electromagnetic structure and deriving a suitable topology. The values of the circuit elements are then determined by an optimization procedure to fit the measured S_{11} to that obtained from the model.

The first step in deriving the equivalent circuit is show in Fig. 7. Circuit elements representing the two parts of the structure and the coupling between them form the starting point. Next a fuller circuit is constructed with resistors added to simulate any loss in the elements and also the radiation resistance of the antenna. Transmission lines were also added since the antenna is essentially a distributed structure and a circuit consisting of only lumped elements will not be accurate enough. The full circuit is shown in Fig. 8. The next step is to run the optimisation procedure to determine the values of the elements. The results of the optimisation gave very small or negligible values for some of the elements and these were eliminated ad the final circuit is shown in Fig. 9.

The resonant circuit represents the outer radiating structure and the transmission line TL2 represents the inner non-radiating structure. The radiation resistance is represented by the 928.9Ω termination, Term2. This of course is not the resistance seen by the input terminals, as the equivalent circuit transforms this resistance to 50Ω at the two transmission frequencies. However, the power in this resistance is the transmitted power from the antenna. The microstrip feed line is represented by TL3. The circuit simulator used does not represent radiation from microstrip so a 5Ω resistor R2 was added for that purpose.

The accuracy of the modelling shown in Fig.10 for both amplitude and phase is very high although it appears in Fig.10b that there is some difference in the phase of the model and measurement. This difference is only due to presentation and if the two phases are unwrapped then the results are very close. Note the difference in the S11 curves between Figs.10a and 7 is caused by the variability of using live test subjects to mount the antennas on.

From the model, the radiated power can be plotted. Figs.11a and b show the power radiated by the radiation resistance and by the microstrip feed respectively for an available input power of 1mW. From Fig.11 it can be determined that the feed radiates out of band, but at 2.4GHz it contributes just 11% of the total radiated power. In the 5GHz band, the maximum feed contribution to radiated power is 15%. A rigorous proof of the results has not been carried out; however the results so far are consistent with measurements and expected performance. An improvement in the microstrip feed matching could increase the total antenna efficiency further.

6.0 CONCLUSION

A dielectric filled dual-band antenna with the overall dimensions of a standard jeans button. The antenna is an improvement of an original design presented in [5] as it has reduced overall size and higher durability. The structure is a dielectric filled cylindrical top loaded monopole which is capacitively coupled to a top disc which in turn is connected to the ground plane by a via pin coaxial to the outer monopole. The button antenna is resonant at both the 2.4GHz and 5.2-5.5GHz WLAN bands. A technique for measuring the permittivity of the textile substrate for frequencies spanning a waveguide band is presented and measured results for Denim and Velcro are given. An equivalent circuit representation of the antenna with lumped elements representing physical capacitances, inductances and losses in the structure was presented. Study of the model allows the radiated power of the antenna to be predicted as a function of frequency and gives insight into the radiation loss from the feeding microstrip line. Good omni-directional patterns are measured with the antenna on a human body and the gain was between 2.65-5.1 dBi within in the matched frequency bands. Finally, this antenna represents an improvement over previous button antenna designs in that the grounded via means the button antenna can be riveted through fabric as a normal jeans button would be.

ACKNOWLEDGEMENT

The authors would like to thank Nigel Simpson, Simon Jakes, Terry Rockhill and Clive Birch for help in the fabrication and measurement of the antennas.

REFERENCES

[1] Lukowicz, P., Büren, T.V., Junker, H., Stäger, M., and Tröster, G.: 'WearNET: "A Distributed Multi-Sensor System for Context Aware Wearables', *in Proc. 4th Int. Conf. On Ubiquitous Computing, Gothenburg,, Sweden, 2002.*

[2] Salonen, P. and Hurme, H.: 'A novel fabric WLAN antenna for wearable applications', *IEEE Antennas and Propagation Society International Symposium*, **2**, June, pp.700-703, 2003.

[3] Tanaka, M. and Jang, J.-H.: 'Wearable microstip antenna', *IEEE antennas and Propagation Society International Symposium* , **2**, pp.704-707, 2003.

[4] Klemm, M., Locher, I. and Tröster, G.: 'A Novel Circularly Polarized Textile Antenna for Wearable Applications' Proc. of 7th European Microwave Week, Amsterdam, Netherlands, pp. 137-140, Oct. 11-14, 2004.

[5] Sanz-Izquierdo, B., Huang, F. and Batchelor, J.C.: 'Covert Dual Band Wearable Button Antenna', Electron. Lett., 2006, **42**, (12), pp.668-670.

[6] Sanz-Izquierdo, B., Huang, F. and Batchelor, J.C.: 'Dual Band Button Antennas for Wearable Applications', IWAT, White Plains, New York, March 6-8, 2006.

[7] Sanz-Izquierdo, B., Miller, J.A., J.C. Batchelor, and M.I. Sobhy, 'Study of Single and Dual Band Wearable Metallic Button Antennas for Personal Area Networks (PANs)', in press for *IET Proceedings on Microwaves, Antennas and Propagation*.

[8] Sanz-Izquierdo, B., Huang, F., Batchelor, J.C. and Sobhy, M.I.: 'Compact Antenna for WLAN on Body Applications', in Proc. 36th European Microwave Week, September 2006.

[9] 'Calculation of the Dielectric Properties of Body Tissues in the Frequency Range 10Hz-100GHz', Nello Carrara, Italian National Research Council, Institute for Applied Physics, Florence, http://niremf.ifac.cnr.it/tissprop/htmlclie/htmlclie.htm.

List of Figures

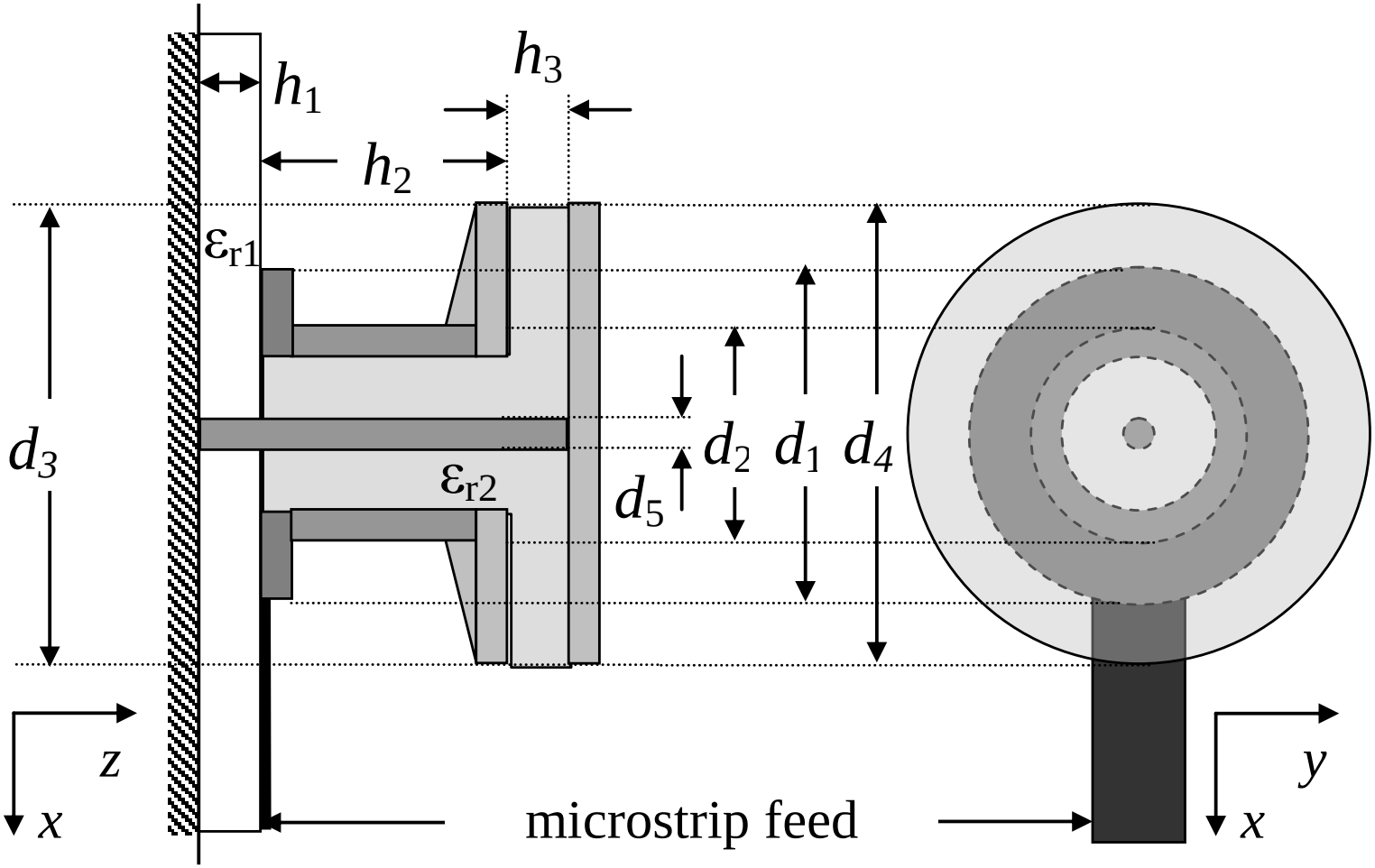

Figure 1: Dual band shorted button structure.

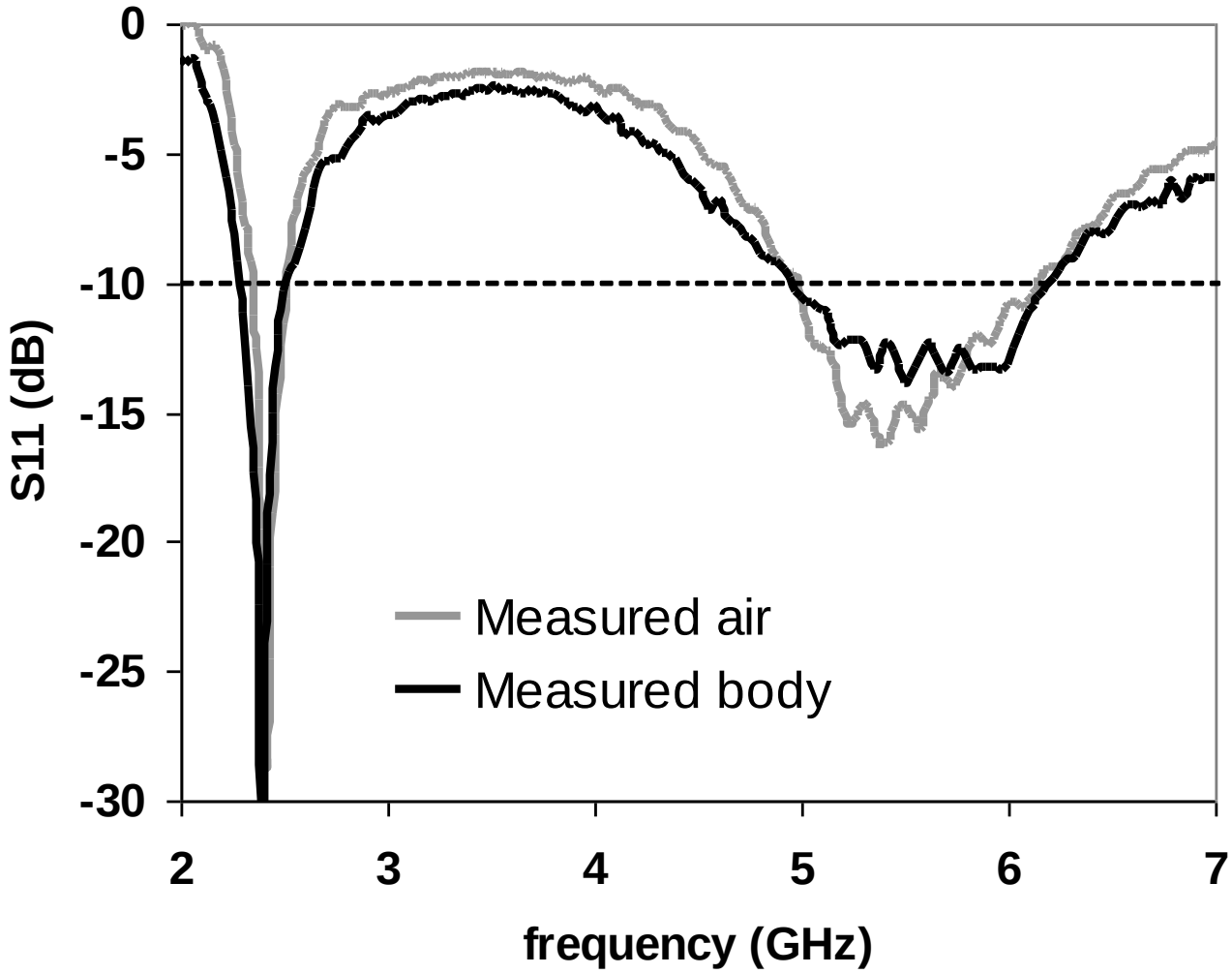

Figure 2: Measured S11 for the Dual Band Shorted Button on and off the human body

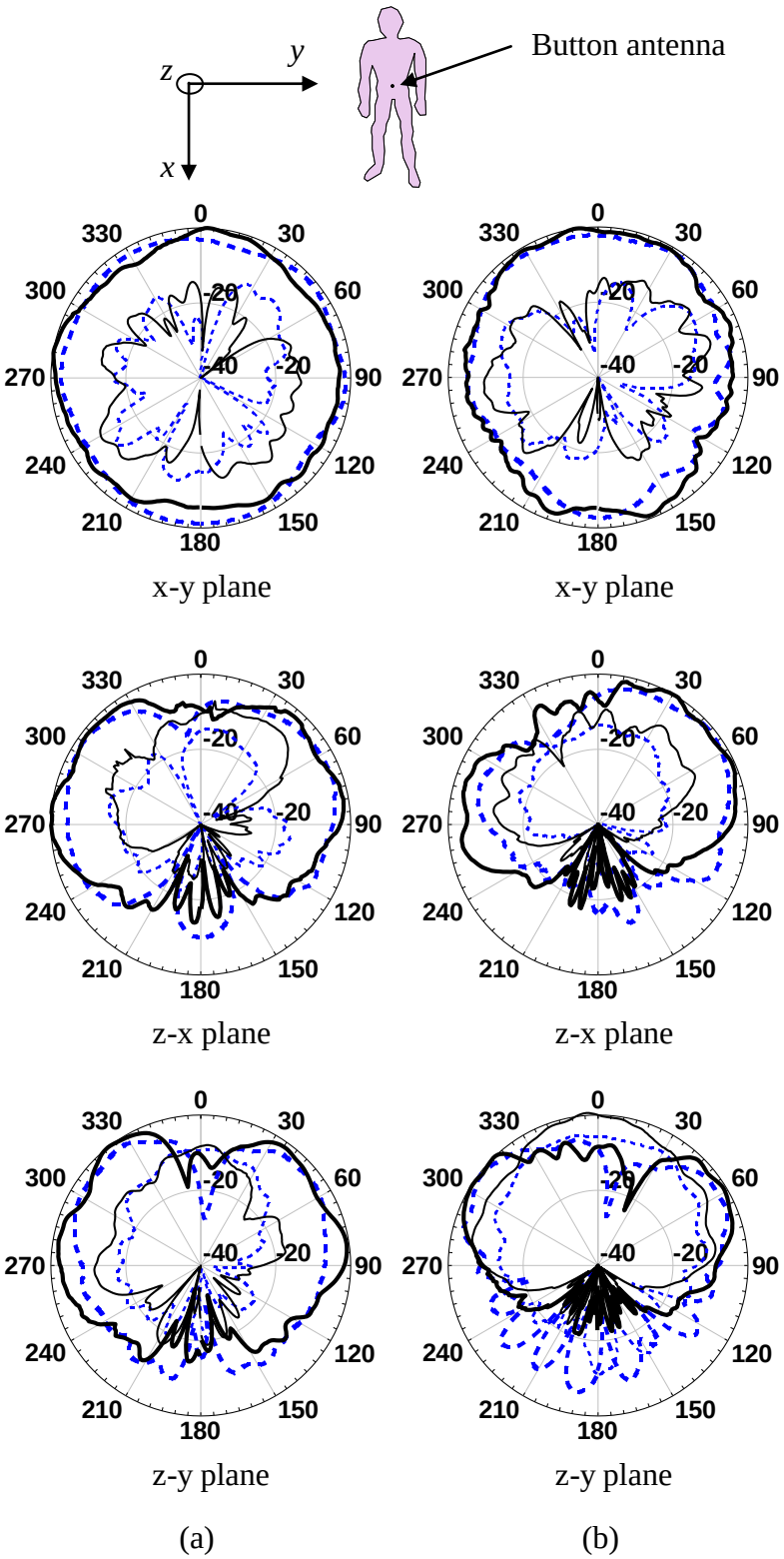

Figure 3: Measured radiation patterns. (a) 2.4GHz, (b) 5.2GHz. Continuous lines are on body measurements. Discontinuous lines are off-body measurements. Heavy line: Co-polarization; thin line: cross polarization.

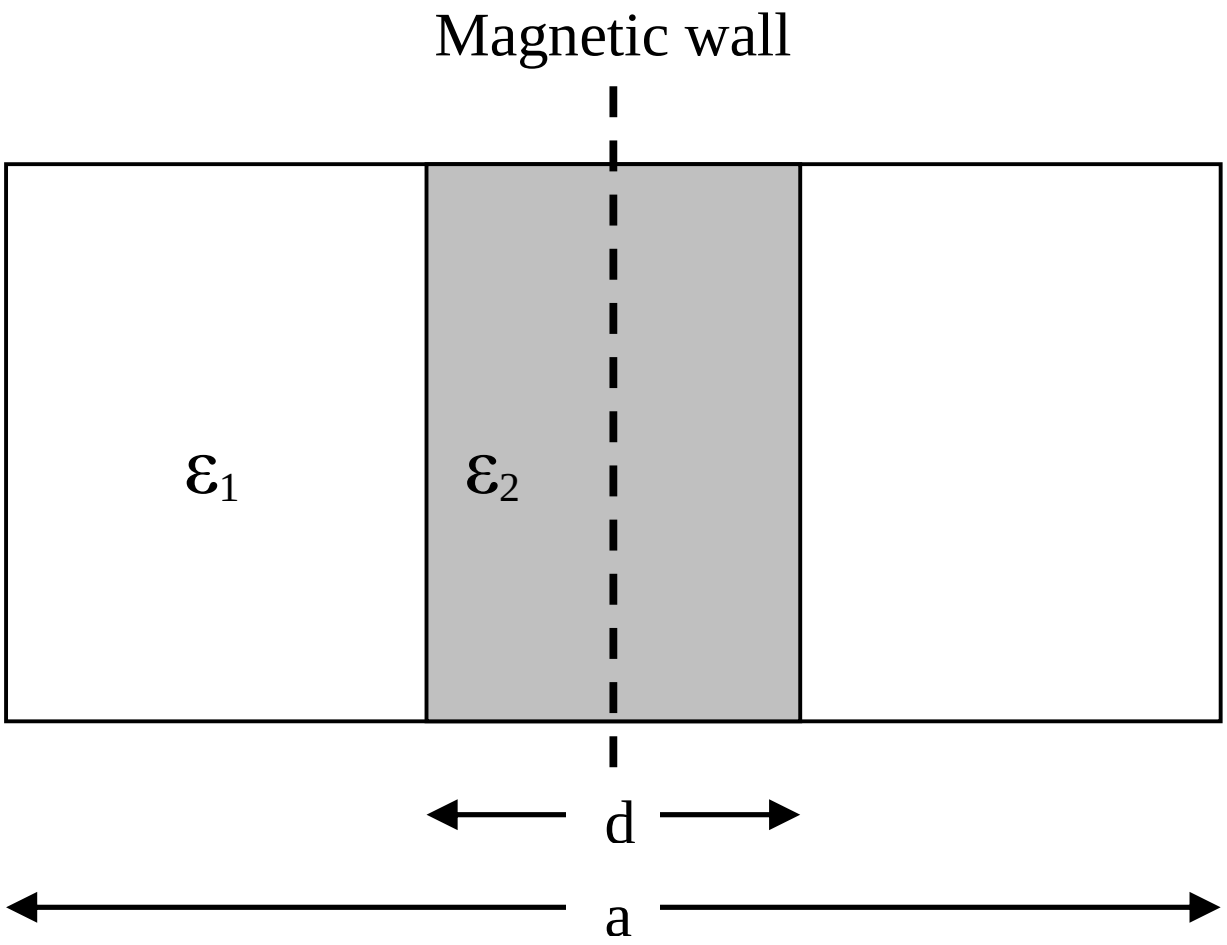

Figure 4: Waveguide cross section width *a* with textile sample width *d*.

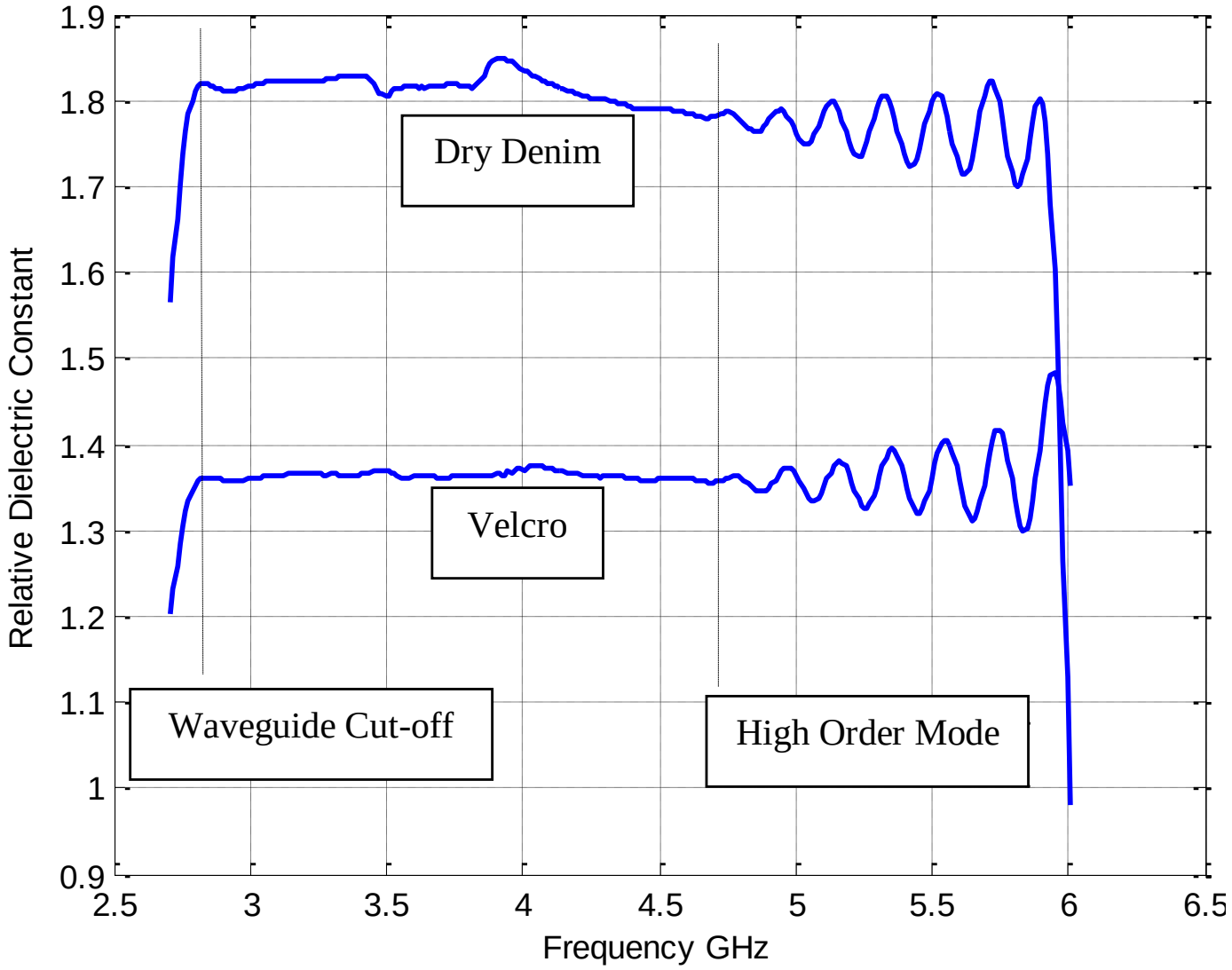

Figure 5: Measured dielectric constant of Velcro and dry Denim.

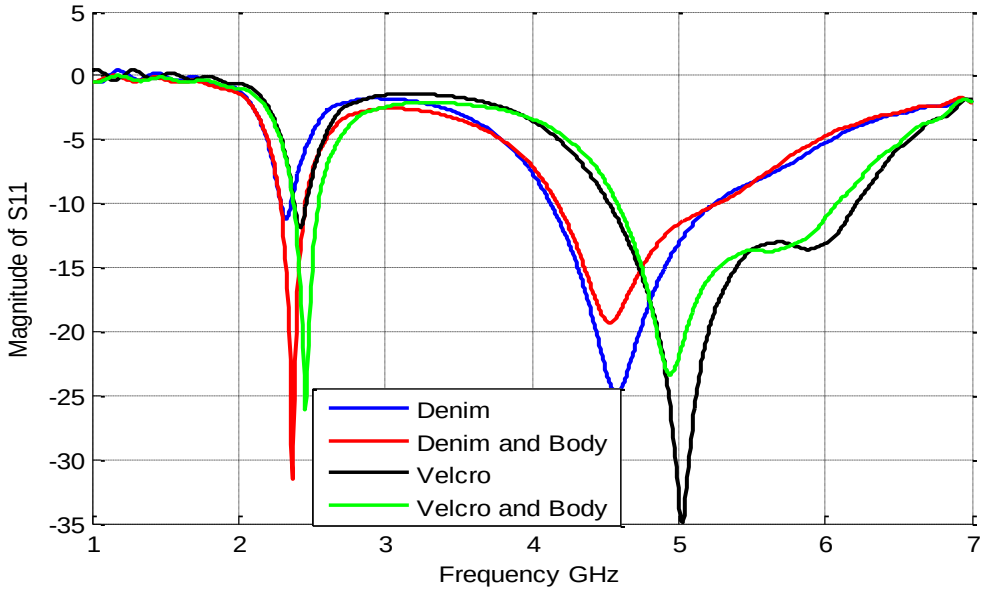

Fig. 6. The effect of including textile materials.

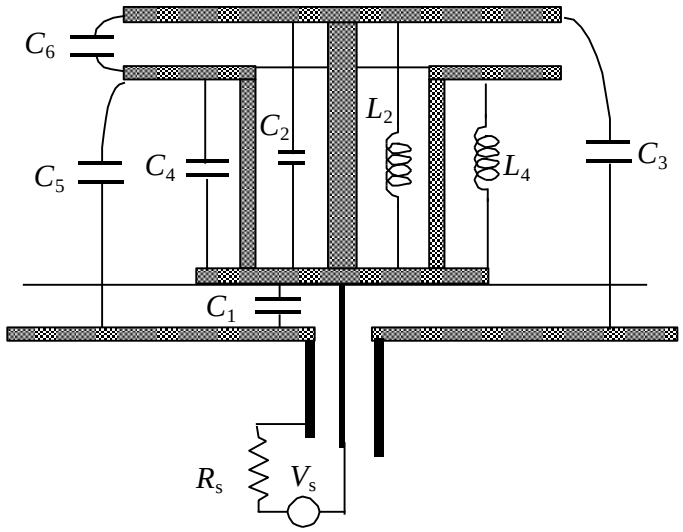

Figure. 7. First step in deriving the equivalent circuit.

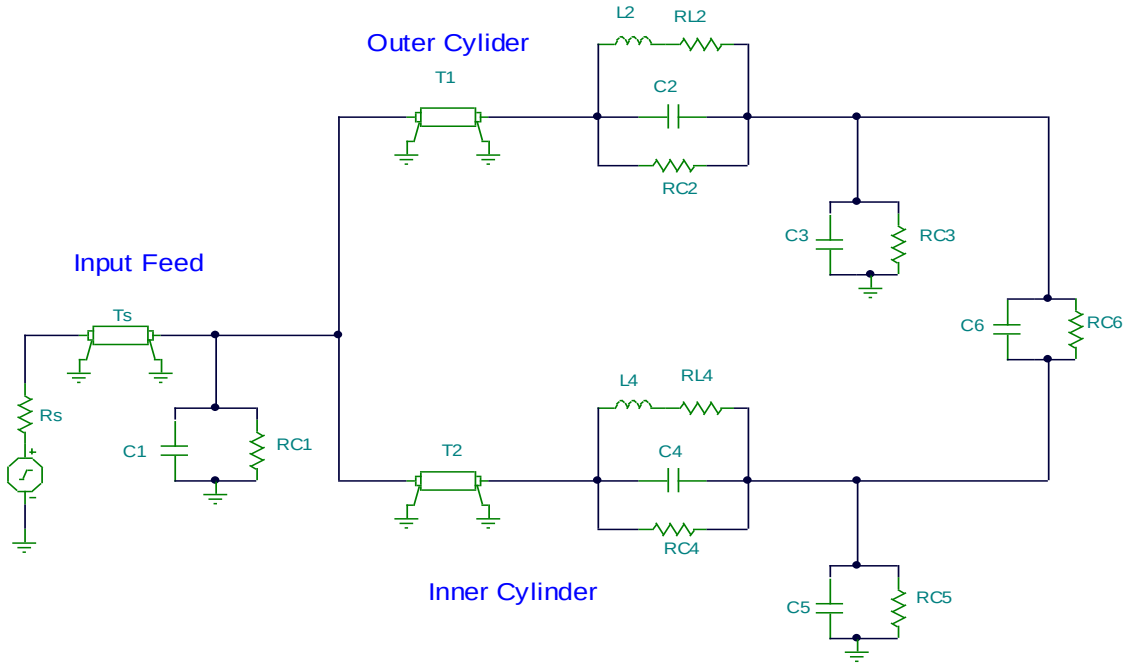

Figure. 8. Full equivalent circuit including losses, radiation and distributed elements.

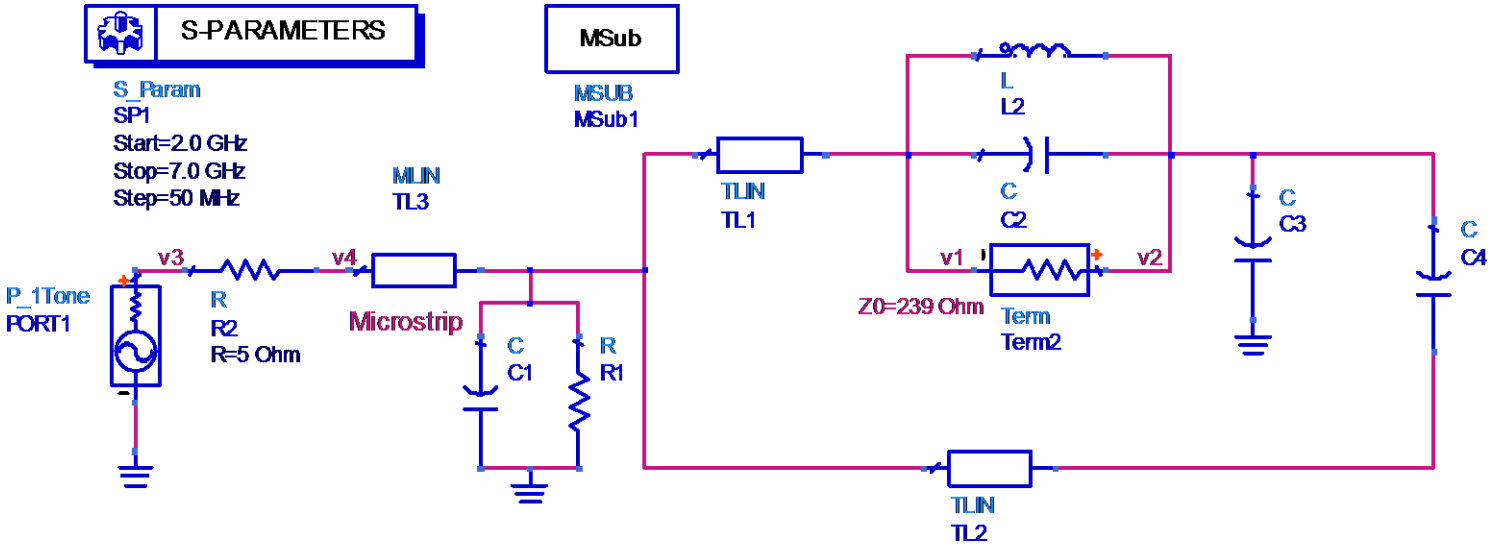

Figure. 9. Final equivalent circuit after eliminating negligible elements.

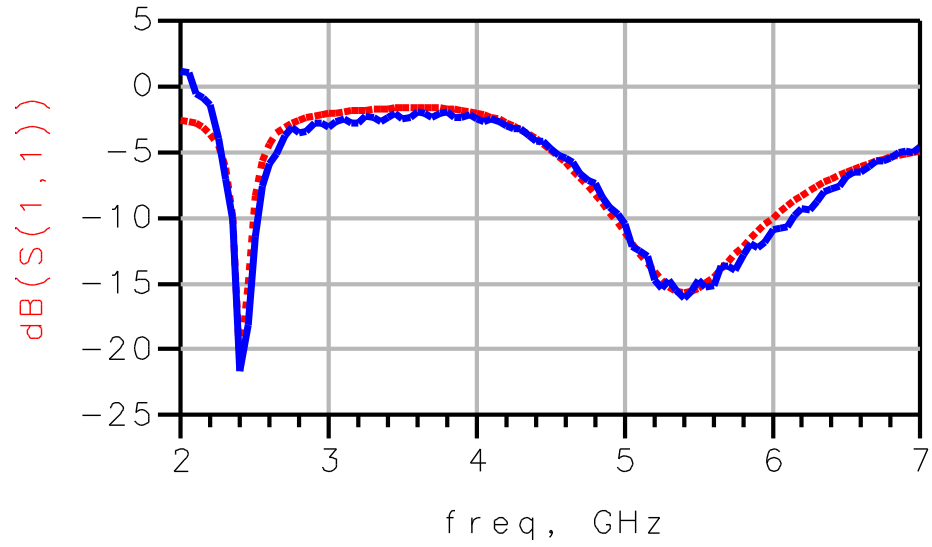

(a)

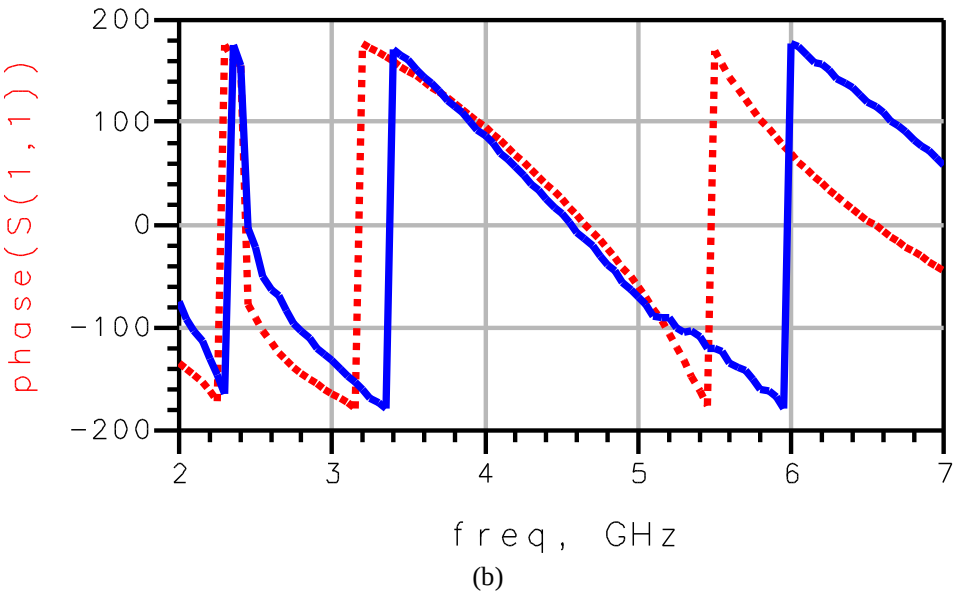

(b)

Figure10: Measured (solid) and modelled (dotted) S_{11} of dual band button antenna. (a) S_{11} Amplitude and (b) S_{11} phase.

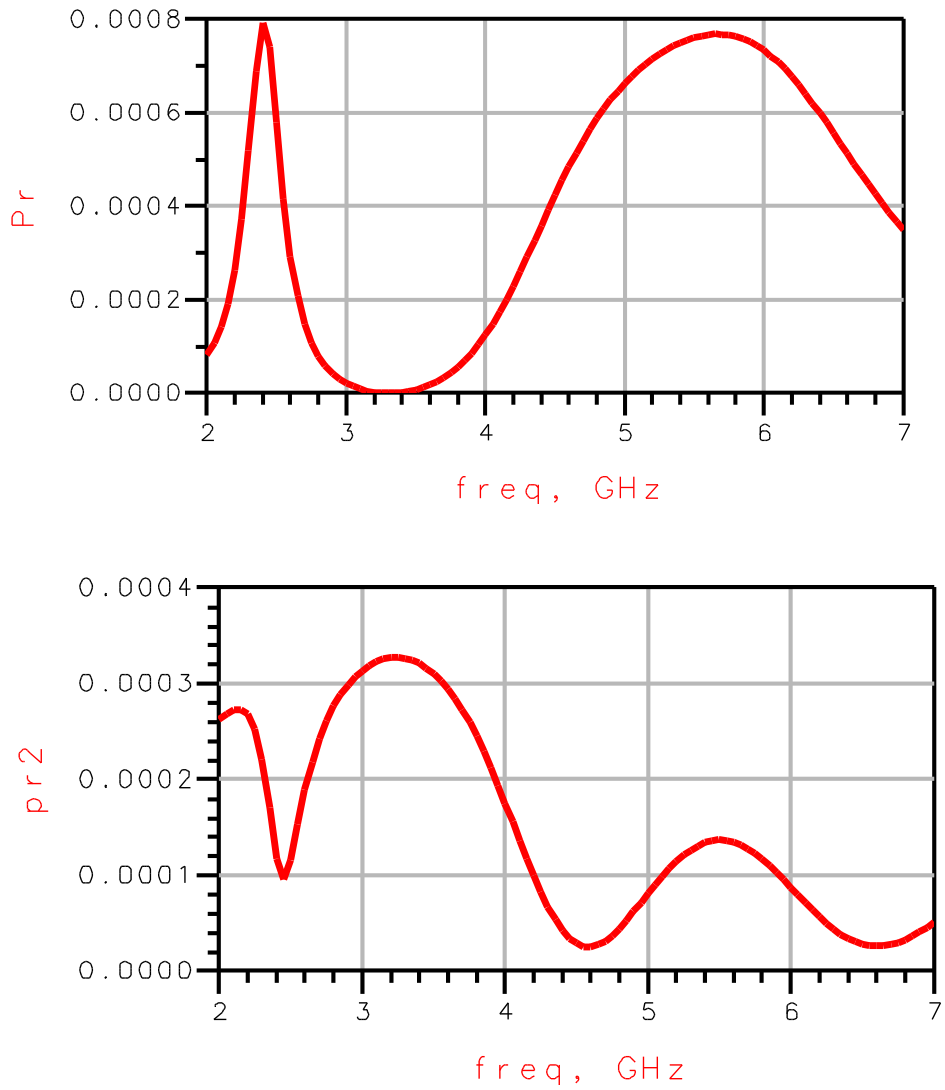

Figure. 11. Radiated power from outer and inner cylinders.